Intra-operative fluorescence-based detection of positive surgical margins during radical prostatectomy: Lessons learned from a pilot ex vivo translational study

Gaelle Fiard, Cecilia Hughes, Redha Heus, Bruno Abert, Emilie Chipon, Isabelle Boudry, Geraldine Saada-sebag, Maysoun Kassem, Cecilia Lanchon, Jean-alexandre Long, et al.

Accepted: 17 December 2022

DOI: 10.1002/lsm.23627

PRECLINICAL STUDY

Intra-operative fluorescence-based detection of positive surgical margins during radical prostatectomy: Lessons learned from a pilot ex vivo translational study

Gaelle Fiard MD, PhD[1,2] | Cecilia Hughes PhD[1,3] | Redha Heus PhD[1,3] | Bruno Abert MSc[1,3] | Emilie Chipon PhD[3,4] | Isabelle Boudry MSc[3,4] | Geraldine Saada-Sebag MD[5] | Maysoun Kassem MD[5] | Cecilia Lanchon MD[2] | Jean-Alexandre Long MD, PhD[1,2] | Jean-Luc Descotes MD, PhD[1,2] | Alexandre Moreau-Gaudry PhD[1,3] | Sandrine Voros PhD[1,4]

[1]CNRS, Grenoble INP, TIMC, Université Grenoble Alpes, Grenoble, France

[2]Department of Urology, Grenoble Alpes University Hospital, Grenoble, France

[3]Université Grenoble Alpes, INSERM, CHU Grenoble Alpes, CIC 1406 (Innovative Technology), Grenoble, France

[4]INSERM, Paris, France

[5]Department of Pathology, Grenoble Alpes University Hospital, Grenoble, France

Correspondence

Gaelle Fiard, Department of Urology, Grenoble Alpes University Hospital, CS 10217, 38043 Grenoble Cedex 9, France.
Email: gfiard@chu-grenoble.fr

Abstract

Objectives: Nerve-sparing techniques during radical prostatectomy have been associated with an increased risk of positive surgical margins. The intra-operative detection of residual prostatic tissue could help mitigate this risk. The objectives of the present study were to assess the feasibility of using an anti-prostate-specific membrane antigen (anti-PSMA) antibody conjugated with a fluorophore to characterize fresh prostate tissue as prostatic or non-prostatic for intra-operative surgical margin detection.

Methods: Fresh prostatic tissue samples were collected from transurethral resections of the prostate (TURP) or prostate biopsies, and either immunolabelled with anti-PSMA antibody conjugated with Alexa Fluor 488 or used as controls. A dedicated, laparoscopy-compliant fluorescence device was developed for real-time fluorescence detection. Confocal microscopy was used as the gold standard for comparison. Spectral unmixing was used to distinguish specific, Alexa Fluor 488 fluorescence from nonspecific autofluorescence.

Results: The average peak wavelength of the immuno-labeled TURP samples ($n = 4$) was 541.7 ± 0.9 nm and of the control samples ($n = 4$) was 540.8 ± 2.2 nm. Spectral unmixing revealed that these similar measures were explained by significant autofluorescence, linked to electrocautery. Three biopsy samples were then obtained from seven patients and also displayed significant nonspecific fluorescence, raising questions regarding the reproducibility of the fixation of the anti-PSMA antibodies on the samples. Comparing the fluorescence results with final pathology proved challenging due to the small sample size and tissue alterations.

Conclusions: This study showed similar fluorescence of immuno-labeled prostate tissue samples and controls, failing to demonstrate the feasibility of intra-operative margin detection using PSMA immuno-labeling, due to marked tissue autofluorescence. We successfully developed a fluorescence device that could be used intraoperatively in a laparoscopic setting. Use of the infrared range as well as newly available antibodies could prove interesting options for future research.

KEYWORDS

fluorescence, laparoscopy, prostate cancer, surgical margin, translational research

INTRODUCTION

Prostate cancer is a major health issue representing over one million cases and the second most common cancer in men worldwide in 2018.[1] The availability of screening using prostate-specific antigen (PSA) testing has led to an increase of localized and locally advanced stages, eligible to curative intent treatments. Among these, radical prostatectomy has shown its oncological safety compared to external beam radiotherapy, but results in significant sexual morbidity in spite of all surgical advances.[2–4] Preoperative staging has considerably improved with the progress of magnetic resonance imaging and targeted biopsy. Still, the degree of nerve-sparing at the time of surgery relies on imprecise imaging features and clinical parameters, put in balance with the priorities of the patient in preserving his sexual function. Nerve-sparing procedures have been associated with an increased risk of positive surgical margins.[5] Positive surgical margins in turn increase the risk of biochemical recurrence and the need for salvage radiotherapy, adding a significant morbidity and cost to the treatment of prostate cancer.[6] Therefore, efforts have been pursued toward the intra-operative detection of positive surgical margins, mostly based on frozen-section histopathology.[7,8] However, in addition to a significant in-procedure wait time, this technique relies on the immediate availability of a trained pathologist. Prostate-specific membrane antigen (PSMA) is expressed in the membrane of all prostate cells, and overexpressed in prostate cancer cells.[9] We present here the initial results and difficulties encountered during a pilot ex vivo translational study evaluating the feasibility of using an anti-PSMA antibody conjugated with a fluorophore to characterize fresh prostate tissue as prostatic or non-prostatic for intra-operative surgical margin detection.

MATERIALS AND METHODS

Tissue collection

After prior assessment of the feasibility of fluorescence measurement on immuno-labeled human adenocarcinoma LNCaP cell lines (unpublished data), two consecutive methods were used to collect fresh prostate tissue samples: (i) tissue was collected from patients who had undergone a transurethral resection of the prostate (TURP samples) and (ii) tissue was collected by biopsy of a radical prostatectomy specimen (biopsy samples). All samples were collected directly from the operating room to ensure that the experiments were carried out on fresh tissue, approaching as much as possible intraoperative conditions. All tissue was collected after written informed consent was obtained and within the context of two clinical trials. Both trials were designed as non-randomized, controlled, open, monocentric trials (ClinicalTrials.gov identifier: NCT02185170 and NCT03157856) and were approved by the relevant ethical committee (Comité de Protection des Personnes, Sud-Est V, France) and by the French National Agency for Medicine and Health Products Safety (Agence Nationale de Sécurité du Médicament et des Produits de Santé—ANSM).

Fluorescence device

A fluorescence device was developed to evaluate tissue intraoperatively during radical prostatectomy.[10] The first prototype is in the form of a testbench (Figure 1), but it is technically feasible to miniaturize the device to make it laparoscopic-compliant.

The device is equipped with a 488 nm wavelength laser source, which is filtered using a BPF 488/10 and then directed into a bidirectional probe positioned

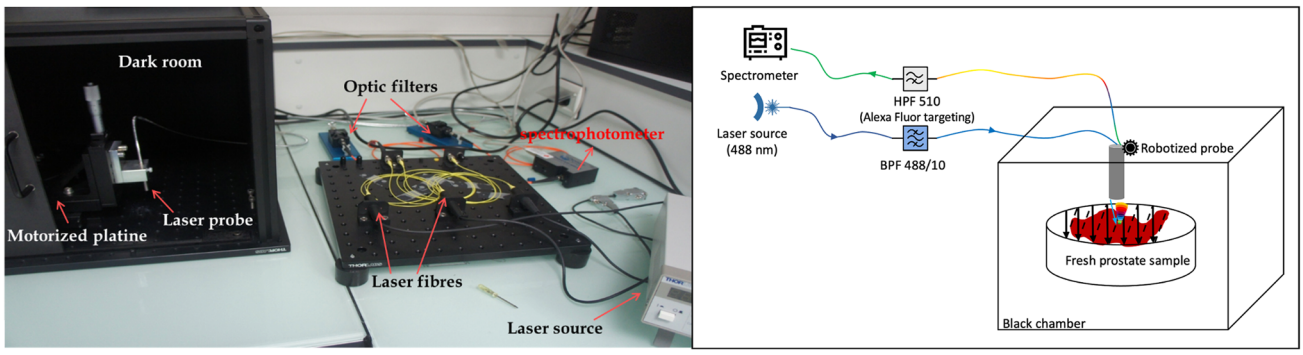

FIGURE 1 The developed fluorescence device prototype: a 488 nm laser source is filtered using a band-pass filter (BPF) 488/10, directed into the probe positioned above the sample in the "dark room." The light collected is filtered using a high-pass filter (HPF) 510 and analyzed using a spectrometer. The position of the probe is controlled using motorized actuators (*x*-, *y*-axis) and a high precision Vernier scale (*z*-axis).

above the sample to be examined. Upon excitation at 488 nm, the Alexa Fluor emits light at 520 nm. Light is collected, filtered using a high-pass filter with a cut-off wavelength of 510 nm (HPF 510), and analyzed using a spectrometer (USB4000 Ocean Optics, 3648-element CCD, range 345–1040 nm). The specifications of the optical fibers—core diameter (Ø), numerical aperture (NA)—are as follows: input Ø = 200 µm, 0.22 NA, and output Ø = 400 µm, 0.39 NA (Thorlabs). For each acquisition, the dimension of the area measured was defined such that the fluorescence of the complete surface of each prostate tissue sample was measured, and the data acquired were post-processed using in-house written MATLAB (MathWorks) software, which enabled the background noise to be removed, the fluorescence spectrum measured at each acquisition point to be smoothed (by convolution with a normalized one-dimensional Gaussian kernel, width = 60) and the peak wavelength of the fluorescence measured at each acquisition point to be calculated.

Furthermore, in-house written MATLAB software was developed to linearly unmix by least-square regression the fluorescence measured using the fluorescence device. The chromophores likely to be present in the fresh prostate tissue samples and which have an excitation spectrum that includes 488 nm were identified as riboflavin, flavin adenine dinucleotide (FAD), lipofuscin, and hemoglobin. The spectra of each of these chromophores was acquired using the fluorescence device or a spectra bank and were modified to take into account the HPF 510 used by the fluorescence device. The unmixing of the fluorescence of every pixel in the image, using the defined subset, was then performed. The percentage of each chromophore present in the sample (mean (m) ± SD (σ) %) was then calculated.

Confocal microscopy

A confocal laser scanning microscope (LSM 710, Zeiss) was used to measure the fluorescence of the prostate tissue samples. The measured fluorescence was considered to be the "gold standard" to which other results are compared. The microscope allows fluorescence to be measured from the surface of the sample to a maximum depth of 200 µm. The fluorescence measurement was acquired using the 488 nm laser source, enabling the signal of the PSMA conjugated with Alexa Fluor 488 (Ex/Em = 488/520 nm) to be measured. For the TURP samples, a band-pass filter (BPF) 520/40 was used. For the biopsy samples, the fluorescence was measured in the range 500–700 nm.

Immuno-labeling method

The immuno-labeling protocol is detailed in Table 1. In brief, samples were washed three times with phosphate-buffered saline (PBS) and then incubated with 1 ml of the anti-PSMA antibody conjugated with Alexa Fluor 488 (Ex/Em = 488/520 nm) in a humidified chamber. The incubation time (45–60 minutes) was chosen as an acceptable intraoperative "waiting time," compatible with the duration of lymph node dissection.

RESULTS

TURP samples

Four TURP samples were examined using the fluorescence device. Two samples were immuno-labeled (anti-PSMA–Alexa Fluor 488) and two samples were used as

TABLE 1 Immuno-labeling protocol

Group	Immuno-labeling	Nuclear staining	Imaging technique	Imaging parameters (filters and wavelengths in nm)
TURP: immuno-labeled ($N = 4$)	Alexa Fluor 488[a] 12 µg/ml, 45 minutes	N/A	Confocal microscope ($N = 2$)	488, BPF 520/40
			Fluorescence device ($N = 2$)	488, BPF 488/10, HPF 510
TURP: control	N/A	N/A	Confocal microscope ($N = 2$)	488, BPF 520/40
			Fluorescence device ($N = 2$)	488, BPF 488/10, HPF 510
Biopsy: immuno-labeled	Alexa Fluor 488[a] 10 µg/ml, 60 minutes	N/A	Confocal microscope ($N = 2$)	488, 500–700 nm
			Fluorescence device ($N = 2$)	488, BPF 488/10, HPF 510
Biopsy: control	N/A	N/A	Confocal microscope ($N = 1$)	488, 500–700 nm
			Fluorescence device ($N = 1$)	488, BPF 488/10, HPF 510

Abbreviations: BPF, band-pass filter; HPF, high-pass filter; TURP, transurethral resections of the prostate.

[a]Exbio mouse anti-human IgG clone GCP-05, Prague, Czech Republic: purchased from CliniSciences.

controls. The fluorescence of the complete surface of each tissue sample was measured. For the immuno-labeled samples, a fluorescence signal with an average peak wavelength of 541.7 ± 0.9 nm was measured. For the control samples, a fluorescence signal very similar to that measured on the immuno-labeled samples was measured, with an average peak wavelength 540.8 ± 2.2 nm. Figure 2 shows the average normalized smoothed fluorescence signal measured using the fluorescence device for each of the control and immuno-marked TURP samples.

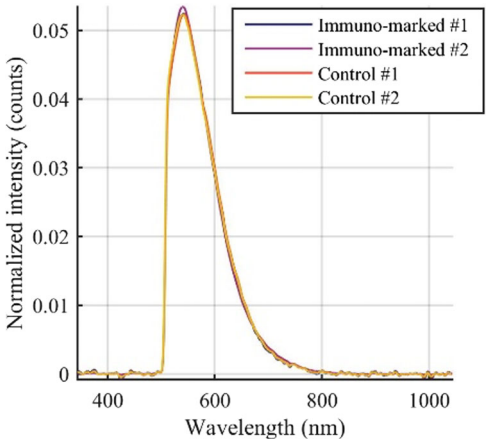

FIGURE 2 Four TURP prostate samples were examined using the fluorescence device: Two immuno-labeled and two controls. The figure shows the average normalized smoothed fluorescence signal measured across the surface of each sample. The average peak wavelength of the immuno-labeled samples was 541.7 ± 0.9 nm and of the control samples was 540.8 ± 2.2 nm. TURP, transurethral resections of the prostate.

Four TURP samples were examined with the confocal microscope using the 488 nm laser source and a BPF 520/40. Two samples were immuno-labeled (anti-PSMA–Alexa Fluor 488) and two samples were used as controls. For both the immuno-labeled samples and the control samples, the peak of the fluorescence measured was situated at approximately 540 nm. Figure 3A shows the fluorescence measured in a zone of an immuno-labeled TURP sample and Figure 3B shows the fluorescence measured in a zone of a control TURP sample.

Both the confocal microscope and fluorescence device results showed no marked difference between the fluorescence measured on the immuno-labeled TURP samples and the fluorescence measured on the control TURP samples. To verify the similarity, the fluorescence measured across one immuno-labeled sample and one control sample was unmixed. For the immuno-labeled TURP sample, the average fluorescence was composed of riboflavin (52.8 ± 19.5%), lipofuscin (25.5 ± 19.6%), and hemoglobin (21.7 ± 13.0%). For the control TURP sample, the average fluorescence was composed of riboflavin (57.0 ± 12.8%), lipofuscin (32.1 ± 10.9%), and hemoglobin (10.9 ± 9.7%). These results are detailed in Table 2 and an image of the spectral unmixing of the immuno-labeled TURP sample is shown in Figure 4. We therefore conclude that the fluorescence measured on the immuno-labeled and control TURP samples was autofluorescence, constituted of riboflavin, lipofuscin, and hemoglobin, with peak wavelength situated at approximately 540 nm, and not PSMA-specific fluorescence. In light of these results, and further experiments using animal tissues confirming that electrocautery was responsible for the signal obtained, the clinical trial was halted. A second clinical trial was started that enabled fresh prostate tissue samples to be collected via biopsy.

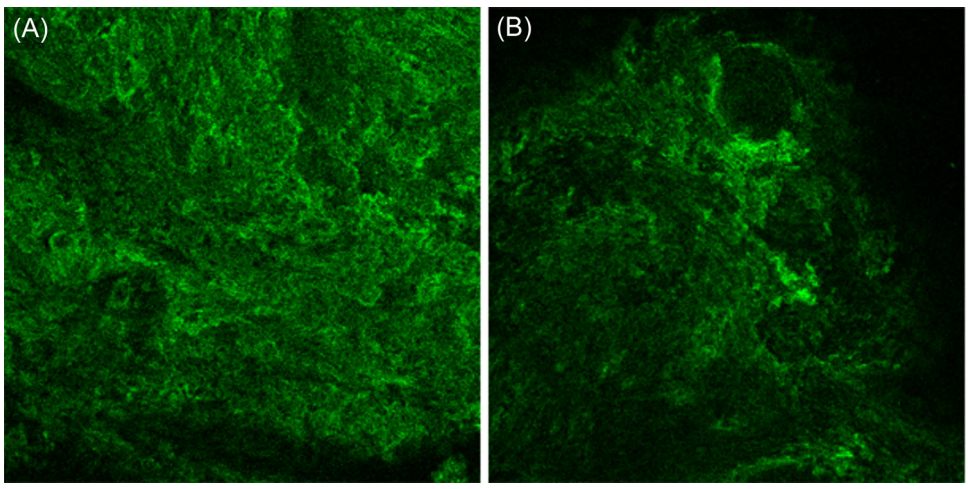

FIGURE 3 Field of (A) an immuno-labeled (anti-PSMA–Alexa Fluor 488) TURP sample and (B) a control TURP sample, measured at the cell surface and at ×10 magnification using the confocal microscope. The peak of the measured fluorescence was located at approximately 540 nm for the immuno-labeled and control TURP sample. Dimensions of the zone = 850 × 850 μm². TURP, transurethral resections of the prostate.

TABLE 2 Representative spectral unmixing for one sample of each group examined

Group	Alexa Fluor 488	Riboflavin	Lipofuscin	Hemoglobin
TURP: immuno-labeled	N/A	52.8 ± 19.5%	25.5 ± 19.6%	21.7 ± 13.0%
TURP: control	N/A	57.0 ± 12.8%	32.1 ± 10.9%	10.9 ± 9.7%
Biopsy: immuno-labeled	24.7 ± 11.3%	75.3 ± 24.4%	N/A	N/A
Biopsy: control	N/A	61.8 ± 18.9%	38.2 ± 15.6%	N/A

Abbreviation: N/A , not applicable; TURP, transurethral resections of the prostate.

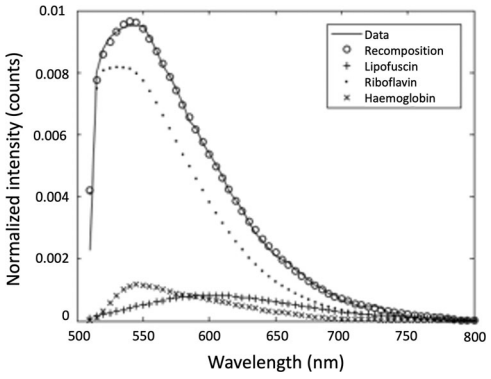

FIGURE 4 Normalized spectral unmixing for an immuno-labeled TURP prostate sample. TURP, transurethral resections of the prostate.

Biopsy samples

Three biopsy samples were obtained from seven patients and examined using both the confocal microscope and the fluorescence device. In each case, two samples were immuno-labeled (anti-PSMA–Alexa Fluor 488) and one sample was used as a control.

The fluorescence of each sample was first measured with the confocal microscope using the 488 nm laser source. The fluorescence was measured in the range 500–700 nm. For the immuno-labeled samples, the fluorescence peak was situated at approximately 521 nm. Figure 5A shows the fluorescence measured in a zone of an immuno-labeled biopsy sample.

The fluorescence of the complete surface of each tissue sample was then measured with the fluorescence device. For the immuno-labeled samples, a fluorescence signal of average peak wavelength 517.0 ± 2.8 nm was measured across the surface of the tissue. For the control sample, a fluorescence signal of average peak wavelength 537.0 ± 7.0 nm was measured across the surface of the tissue. Figure 5B shows the fluorescence measured across the surface of an immuno-labeled biopsy sample.

Spectral unmixing of one of the immuno-labeled biopsy samples shows that the fluorescence was composed of Alexa Fluor 488 (24.7 ± 11.3%) and riboflavin (75.3 ± 24.4%). For the control biopsy sample, the fluorescence was composed of riboflavin (61.8 ± 18.9%) and lipofuscin (38.2 ± 15.6%). Please see Table 2 and Figure 5C.

All other samples, using the same experimental conditions, also showed significant nonspecific fluorescence using both confocal microscopy and the fluorescence device. Indeed, observation under the confocal microscope displayed diffuse fluorescence in the fibromuscular tissue, raising questions regarding the reproducibility of the fixation of the anti-PSMA antibodies on the samples. As this phenomenon did not appear on preliminary experiences on cell lines, and the rinsing protocol was thorough, we could not explain this behavior. Comparing the results obtained with final pathology also proved difficult for the pathologists given the size of the specimens involved and tissue alterations following the incubation/tagging protocol.

DISCUSSION

We present here the attempted translational use of an anti-PSMA antibody conjugated with a fluorophore to characterize fresh prostate tissue as prostatic or non-prostatic for intra-operative surgical margin detection. The obtention of fresh prostatic tissue mimicking the actual intra-operative conditions required significant efforts and the set-up of two consecutive clinical trials and the absence of significant finding due to the significant autofluorescence of tissues can be perceived as disappointing. However, a lot has been learned during the process and will be used to steer future research.

Firstly, the autofluorescence of prostatic tissue consecutive to electrocautery when using TURP samples had been largely overlooked, and kept interfering with fluorescence measurements even after TURP chips had been resliced. This finding had been reported by Vo et al.[11] on burnt skin, which when illuminated with blue light (488 nm), demonstrated a marked autofluorescence, while no autofluorescence was detected in control (unburnt) tissue. Nevertheless, if used intraoperatively, some degree of electrocautery is to be expected and the choice of another emission wavelength (e.g., in the infrared range) could help address this issue. At the beginning of this project, we made the choice to use commercially available anti-PSMA antibodies conjugated with fluorophores, to avoid the additional burden of tagging the antibodies ourselves. The choice of commercially available solutions was scarce at the time, but more options would be available today (e.g., anti-PSMA

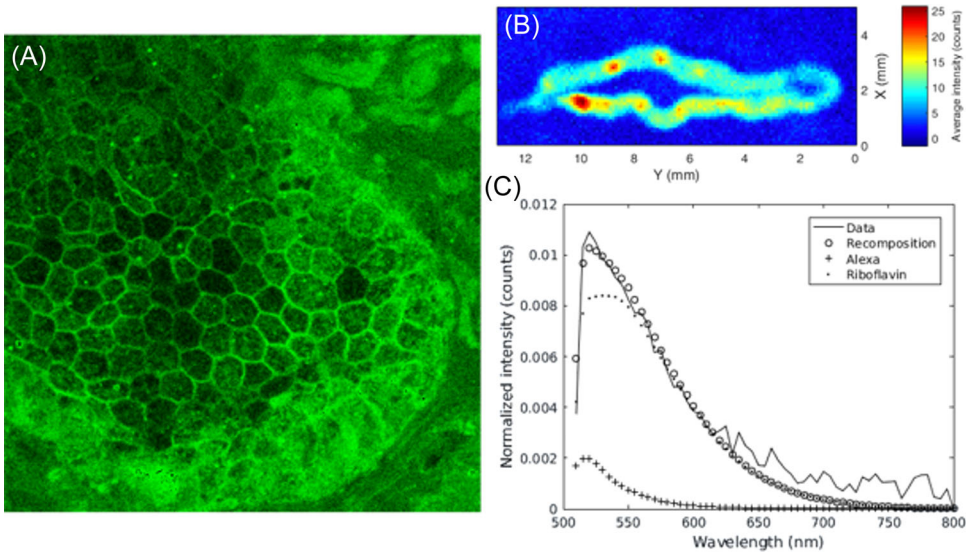

FIGURE 5 Immuno-labeled biopsy sample: (A) field of the sample measured at the cell surface and at ×63 magnification using the confocal microscope, dimensions of the zone = 135 × 135 μm²; (B) fluorescence of the sample measured using the fluorescence device; (C) normalized spectral unmixing of the sample shows that the fluorescence measured was composed of Alexa Fluor 488 and riboflavin.

antibody conjugated with Alexa Fluor 750). In any case, to our knowledge, no anti-PSMA antibody conjugated with a fluorophore is validated for intra-operative use on humans, and one objective of this feasibility study would have been, if successful, to support further validation steps during surgical procedures in animal models and humans.

Secondly, more recent studies published after the design of our initial protocol raised specificity issues of PSMA as a prostatic tissue marker. Chaux et al. looked at the expression of PSMA in prostatectomy specimens specifically studying its expression in neurovascular bundle elements resected with the prostate. Unfortunately, they demonstrated that ganglionic cells found in prostatic neurovascular bundles could also be positive for PSMA, reducing its interest in the specific indication of residual prostatic tissue detection.[12] Furthermore, some prostate cancers may not express PSMA.[13]

Thirdly, we had initially planned to detect variations in fluorescence intensity depending on the presence of prostatic adenocarcinoma in the resected samples, and the clinical trial was designed to allow for the obtention of samples with a high and low probability of harboring adenocarcinoma (based on PSA levels, digital rectal examination, and prostatic magnetic resonance imaging). Although the intensity of autofluorescence encountered prevented us from any comparison, we have to acknowledge that defining the "ground truth," that is, obtaining the final pathology of each sample after it went through all the experimental steps, proved critically challenging.

Another translational aspect of this study that has been overlooked in our protocol was the actual surgical field, and the presence of fluid or blood that could prevent any immunolabelling. Intraoperative detection of surgical margins in the pelvis is therefore in direct concurrence with techniques analyzing the prostate sample outside the operating field.[14] Among these, the NeuroSAFE technique, based on a standardized frozen section examination of the prostate specimen, has demonstrated an impact on the reduction of positive surgical margins in spite of increased use of nerve-sparing techniques, resulting in improved potency outcomes.[15] The intraoperative wait time was reduced to 35 ± 12 minutes with a trained team and pathologist for robot-assisted radical prostatectomy, and could be used for lymphadenectomy and vesico-urethral anastomosis.[16]

Our study is not without limitations. Many choices made in the design of the study and antibody selection are explained by a lack of evidence at the time the study was set up. The limited number of patients and specimens included limit the power of the results obtained but also highlight the difficulties of translational research and the necessity of constant experimental adjustments based on the findings obtained, which can lead to significant additional time and cost for the design of a new protocol, to respect ethical considerations. We still learned a lot from these two apparently unsuccessful clinical trials. First of all, we were able to develop and successfully use a fluorescence device that could be used intraoperatively in a laparoscopic setting. We can now focus our future experiments on other more specific tumor markers and know that the infrared range would be better suited to avoid any interference with tissue autofluorescence. Finally, we also know that to be able to directly concurrence intraoperative frozen section examination, a wait time of maximum 40 minutes will be required, as well as the ability to analyze a non-dry surgical field.

This attempted translational use of an anti-PSMA antibody conjugated with a fluorophore to characterize fresh prostate tissue as prostatic or non-prostatic for intra-operative surgical margin detection failed to demonstrate its feasibility. Despite significant collaborative efforts and two consecutive clinical trials for the obtention of fresh prostatic tissue mimicking the actual intra-operative conditions, marked tissue autofluorescence prevented the comparison of PSMA immunolabeling between prostatic and non-prostatic tissue. Still, we were able to develop and successfully use a fluorescence device that could be used intraoperatively in a laparoscopic setting. Use of another emission wavelength (e.g., in the infrared range) could help address the interference with autofluorescence, as well as the use of newly-available commercial or custom anti-PSMA antibodies. Finally, to be able to directly concurrence intraoperative frozen section examination, a wait time of maximum 40 minutes will be required, as well as the ability to analyze a nondry surgical field.

ACKNOWLEDGMENT

The authors wish to thank Yves Usson, Marie-Paule Montmasson, and Françoise Giroud for their help.

CONFLICT OF INTEREST

The authors declare no conflict of interest.

ORCID

Gaelle Fiard http://orcid.org/0000-0003-3049-5318

REFERENCES

1. Bray F, Ferlay J, Soerjomataram I, Siegel RL, Torre LA, Jemal A. Global cancer statistics 2018: GLOBOCAN estimates of incidence and mortality worldwide for 36 cancers in 185 countries. CA Cancer J Clin. 2018;68(6):394–424. https://doi.org/10.3322/caac.21492
2. Hamdy FC, Donovan JL, Lane JA, Mason M, Metcalfe C, Holding P, et al. 10-year outcomes after monitoring, surgery, or radiotherapy for localized prostate cancer. N Engl J Med. 2016;375(15):1415–24. https://doi.org/10.1056/NEJMoa1606220
3. Donovan JL, Hamdy FC, Lane JA, Mason M, Metcalfe C, Walsh E, et al. Patient-reported outcomes after monitoring, surgery, or radiotherapy for prostate cancer. N Engl J Med. 2016;375(15):1425–37. https://doi.org/10.1056/NEJMoa1606221
4. Capogrosso P, Vertosick EA, Benfante NE, Eastham JA, Scardino PJ, Vickers AJ, et al. Are we improving erectile function recovery after radical prostatectomy? Analysis of patients treated over the last decade. Eur Urol. 2019;75(2):221–8. https://doi.org/10.1016/j.eururo.2018.08.039
5. Soeterik TFW, van Melick HHE, Dijksman LM, Stomps S, Witjes JA, van Basten JPA. Nerve sparing during robot-assisted radical prostatectomy increases the risk of ipsilateral positive surgical margins. J Urol. 2020;204(1):91–5. https://doi.org/10.1097/JU.0000000000000760
6. Martini A, Marqueen KE, Falagario UG, Waingankar N, Wajswol E, Khan F, et al. Estimated costs associated with radiation therapy for positive surgical margins during radical prostatectomy. JAMA Network Open. 2020;3(3):e201913. https://doi.org/10.1001/jamanetworkopen.2020.1913
7. Schlomm T, Tennstedt P, Huxhold C, Steuber T, Salomon G, Michl U, et al. Neurovascular structure-adjacent frozen-section examination (NeuroSAFE) increases nerve-sparing frequency and reduces positive surgical margins in open and robot-assisted laparoscopic radical prostatectomy: experience after 11,069 consecutive patients. Eur Urol. 2012;62(2):333–40. https://doi.org/10.1016/j.eururo.2012.04.057
8. Dinneen EP, Van Der Slot M, Adasonla K, Tan J, Grierson J, Haider A, et al. Intraoperative frozen section for margin evaluation during radical prostatectomy: a systematic review. Eur Urol Focus. 2020;6(4):664–73. https://doi.org/10.1016/j.euf.2019.11.009
9. Olivier J, Stavrinides V, Kay J, Freeman A, Pye H, Ahmed Z, et al. Immunohistochemical biomarker validation in highly selective needle biopsy microarrays derived from mpMRI-characterized prostates. Prostate. 2018;78(16):1229–37. https://doi.org/10.1002/pros.23698
10. Voros S, Moreau-Gaudry A, Tamadazte B, Custillon G, Heus R, Montmasson MP, et al. Devices and systems targeted towards augmented robotic radical prostatectomy. IRBM. 2013;34(2):139–46. https://doi.org/10.1016/j.irbm.2013.01.014
11. Vo LT, Anikijenko P, McLaren WJ, Delaney PM, Barkla DH, King RG. Autofluorescence of skin burns detected by fiber-optic confocal imaging: evidence that cool water treatment limits progressive thermal damage in anesthetized hairless mice. J Trauma: Injury Infect Crit Care. 2001;51(1):98–104. https://doi.org/10.1097/00005373-200107000-00016
12. Chaux A, Eifler J, Karram S, Al-Hussain T, Faraj S, Pomper M, et al. Focal positive prostate-specific membrane antigen (PSMA) expression in ganglionic tissues associated with prostate neurovascular bundle: implications for novel intraoperative PSMA-based fluorescent imaging techniques. Urol Oncol. 2013;31(5):572–5. https://doi.org/10.1016/j.urolonc.2011.04.002
13. Paschalis A, Sheehan B, Riisnaes R, Rodrigues DN, Gurel B, Bertan C, et al. Prostate-specific membrane antigen heterogeneity and DNA repair defects in prostate cancer. Eur Urol. 2019;76(4):469–78. https://doi.org/10.1016/j.eururo.2019.06.030
14. Olde Heuvel J, de Wit-van der Veen BJ, Huizing DMV, van der Poel HG, van Leeuwen PJ, Bhairosing PA, et al. State-of-the-art intraoperative imaging technologies for prostate margin assessment: a systematic review. Eur Urol Focus. 2021;7:733–41. https://doi.org/10.1016/j.euf.2020.02.004
15. Mirmilstein G, Rai BP, Gbolahan O, Srirangam V, Narula A, Agarwal S, et al. The neurovascular structure-adjacent frozen-section examination (NeuroSAFE) approach to nerve sparing in robot-assisted laparoscopic radical prostatectomy in a British setting—a prospective observational comparative study. BJU Int. 2018;121(6):854–62. https://doi.org/10.1111/bju.14078
16. Beyer B, Schlomm T, Tennstedt P, Boehm K, Adam M, Schiffmann J, et al. A feasible and time-efficient adaptation of NeuroSAFE for da Vinci robot-assisted radical prostatectomy. Eur Urol. 2014;66(1):138–44. https://doi.org/10.1016/j.eururo.2013.12.014

How to cite this article: Fiard G, Hughes C, Heus R, Abert B, Chipon E, Boudry I, et al. Intra-operative fluorescence-based detection of positive surgical margins during radical prostatectomy: Lessons learned from a pilot ex vivo translational study. Lasers Surg Med. 2022;1–7. https://doi.org/10.1002/lsm.23627